



Rathke Pouch Cyst

Raquel del Carpio-O'Donovan, Hoang Duong

Stereoscopic Stereotaxy

page 3

Glial Tumors

Pseudotumor Cerebri

page 7

The Brain Isaac Asimov

page 8

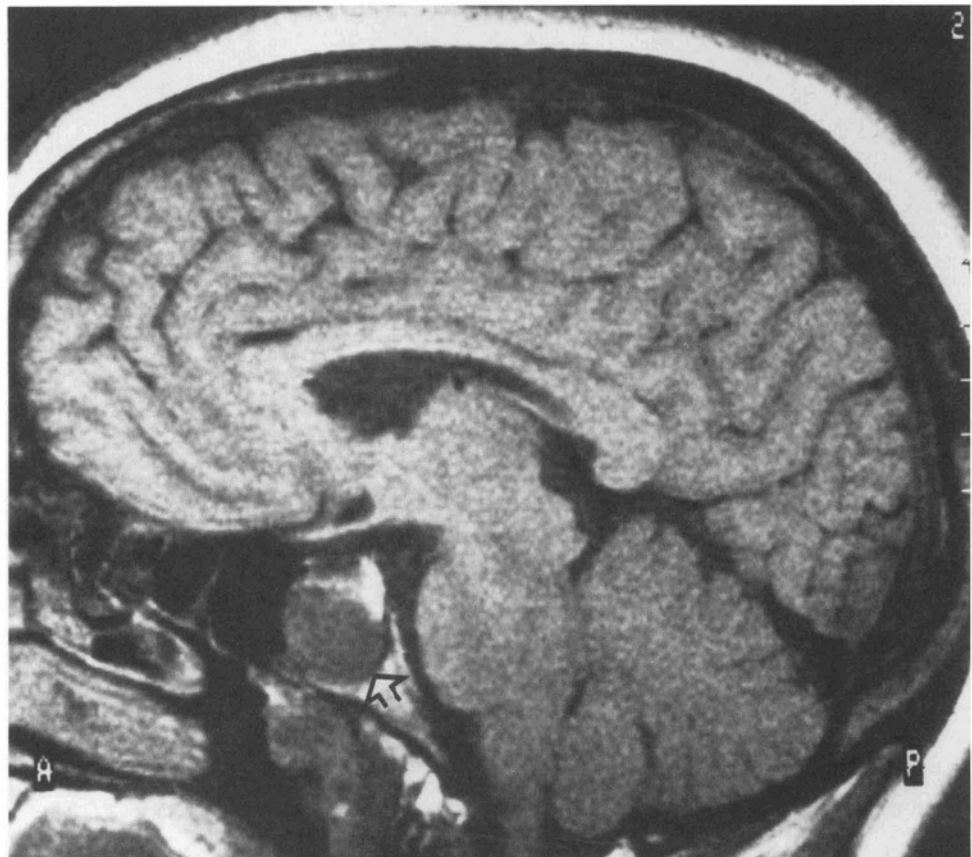


Figure 1 - MRI, sagittal SE 600/20. Intrasellar hypointense mass extending into sphenoid sinus (arrow). Pituitary gland elevated, optic nerve not involved.

(article on page 2)

A 48 year old woman had an MRI examination of the brain which confirmed the clinical diagnosis of multiple sclerosis. Incidentally, a cystic mass was noted in the sella turcica. A pharyngeal soft tissue mass containing cysts was also shown (Figs. 1, 2). A contrast enhanced CT scan additionally showed a diagonal conduit in the basisphenoid joining the pharyngeal mass to the cyst (Figs. 3, 4). Removal of this lesion was done via transphenoidal approach. Amber fluid was aspirated from a thin walled cyst. Its wall was partially excised. The histopathological diagnosis was Rathke pouch cyst.

Rathke pouch is a diverticulum of the primitive oral ectoderm which anterior and posterior walls are precursors of the anterior lobe of the pituitary gland. A central portion or cleft may in some instances expand, giving origin to Rathke cysts. A spectrum of developmental disorders occurring in this area include craniopharyngiomas as the most complex ones, while Rathke cysts represent the simplest form.

The CT and MR imaging findings consistently show a well defined, midline mass in the sella turcica with extension into the suprasellar cistern or into the sphenoid sinus. The density on CT and intensity on MRI are varied (1) depending on the protein concentration in the cyst.

In our case, the cyst had a CSF-like signal, related to low protein concentration. The diagonal conduit seen in the basisphenoid represents persistence of

the craniopharyngeal canal. This bony defect associated with a nasopharyngeal mass has been described with ectopia of the pituitary and other anomalies of the nose and palate (2), gigantism (3) and mostly with meningoencephaloceles (4).

Usually asymptomatic and, as in the present case, a serendipitous finding, Rathke cysts may attain large size and compress the chiasma, hypothalamus and pituitary gland.

The usual differential diagnosis is with craniopharyngioma, arachnoid cyst and cystic pituitary adenoma (1).

Bibliography

- (1) Kucharczyk W et al. Rathke cleft cysts: CT, MR imaging and pathologic features. *Radiology* 165:491-495; 1987.
- (2) Tweedie AR, Keith A. Ectopia of the pituitary, with other congenital anomalies of the nose, palate and upper lip. *JR Soc Med Laringol* 4:47-54; 1910-11.
- (3) Behrens LH, Barr DP. Hyperpituitarism beginning in infancy: the Alton giant. *Endocrinology* 16:120-128; 1932.
- (4) Pollock JA et al. Transphenoidal and transthemoidal encephaloceles: a review of clinical and roentgen features in 8 cases. *Radiology* 90:442-453; 1968.

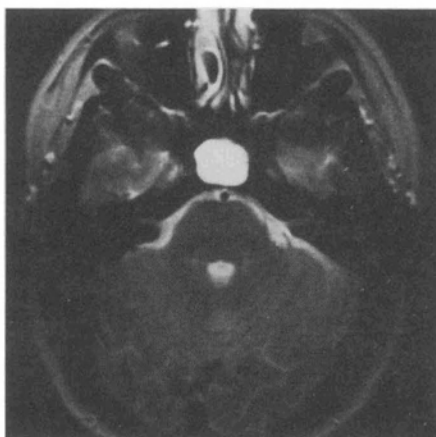


Figure 2— MRI axial SE 2100/80. Homogeneous hyperintense sellar mass.

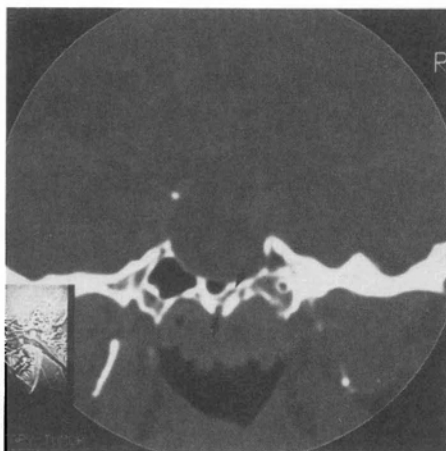


Figure 3- CT, coronal, bone window: Diagonal conduit extending from the floor of the sella to the undersurface of the basisphenoid.

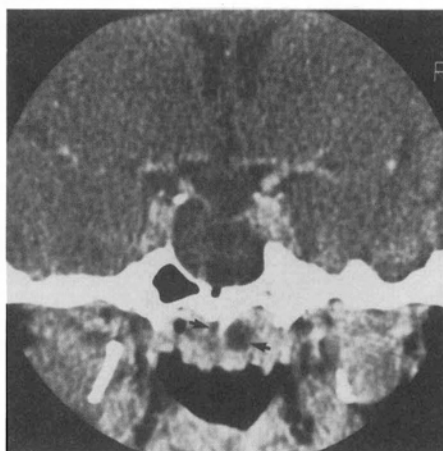


Figure 4 — CT, coronal, soft tissue window. Nasopharyngeal mass cysts. Expanded sella turcica with hypodense mass.

Integrated Three-dimensional and Stereoscopic Imaging for Stereotactic Neurosurgery Planning

T M Peters^{1 2}, C Henri¹, L Collin¹, B Pike¹ and A Olivier³
NeuroImaging Laboratory¹, Dept. of Radiology², and Dept. of Neurosurgery³,

Montreal Neurological Institute,
3801 University St., Montreal, Quebec H3A-2B4, Canada

Introduction

Stereotactic neurosurgery planning, an intrinsically three-dimensional procedure, is generally performed on the basis of two-dimensional tomographic or projection images¹. We present extensions to these conventional procedures that use stereoscopic digital subtraction angiography, three-dimensional

volume rendered computed tomography or magnetic resonance images, or a combination of these modalities. The stereoscopic DSA images are analysed interactively on a 3-D workstation. This system employs a liquid-crystal polarizing shutter to display alternate left-and right-eye views to a user wearing polarized glasses.

Quantitative planning operations

may be performed on the basis of the angiograms alone, or in conjunction with tomographic images of the anatomy. We also present examples of volume-rendered three-dimensional images from MR data sets, along with stereoscopic angiograms that have been combined with volumetric anatomical images.

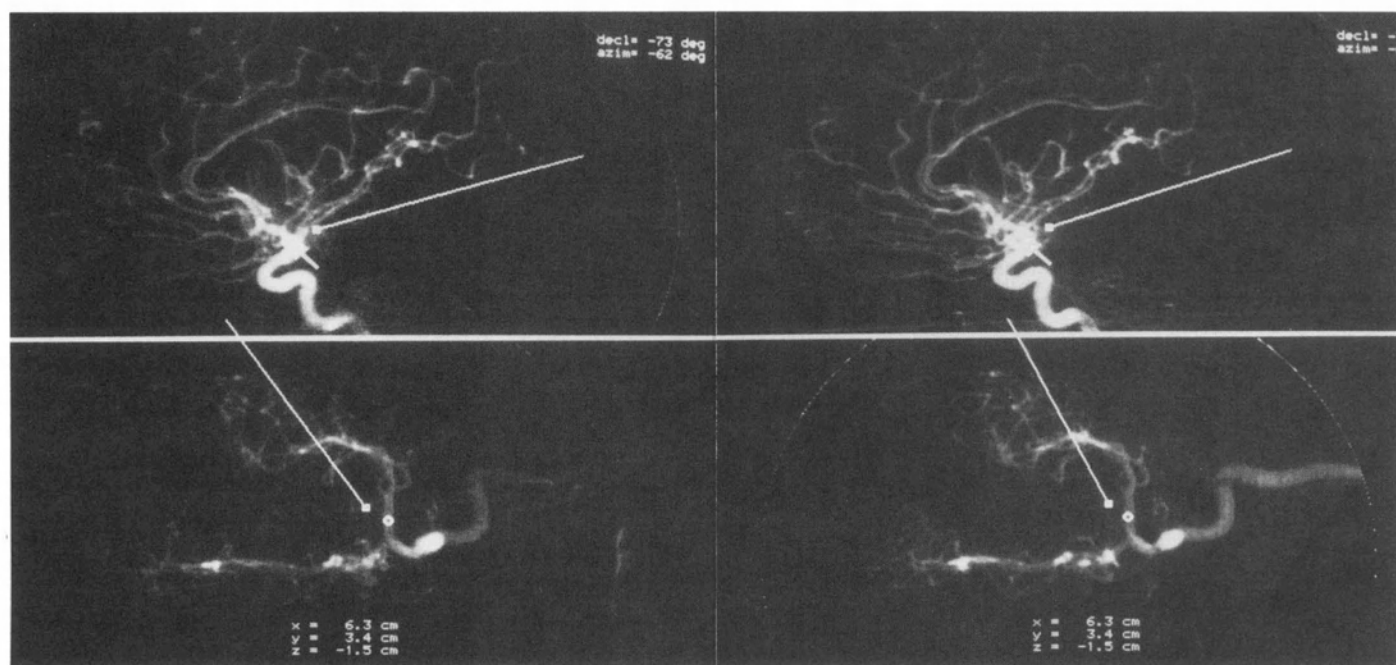


Figure 1

Clinical Examples

Figure 1 shows a stereoscopic pair of DSA images as seen on the stereoscopic workstation. They may be viewed here by crossing the eyes. On the computer screen they appear overlaid, but may be resolved in depth by viewing them using polarized glasses. In this image set, we see a stereotactic probe positioned in each image, as well as a point (a circle in the lower image and an arrow in the upper) marked on the middle cerebral artery.

Figure 2 demonstrates an alternative display in which the CT slice at the level of the cursor is displayed in the lower left-hand corner of the image. Here the movement of the 3-D cursor (which is manipulated by the operator using a mouse) within the volume defined by the

angiograms is reflected in the CT slice. Note that this image shows the overlaid left-and right-eye views superimposed. This is what the observer sees without the polarized glasses.

In Figure 3 we see a 'volume-rendered' MR image, after

processing on our PIXAR image computer. The original data set is 64 T1-weighted MR slices, which have been pre-processed by the removal of a wedge-shaped segment in order to visualize the region of interest.



Figure 3

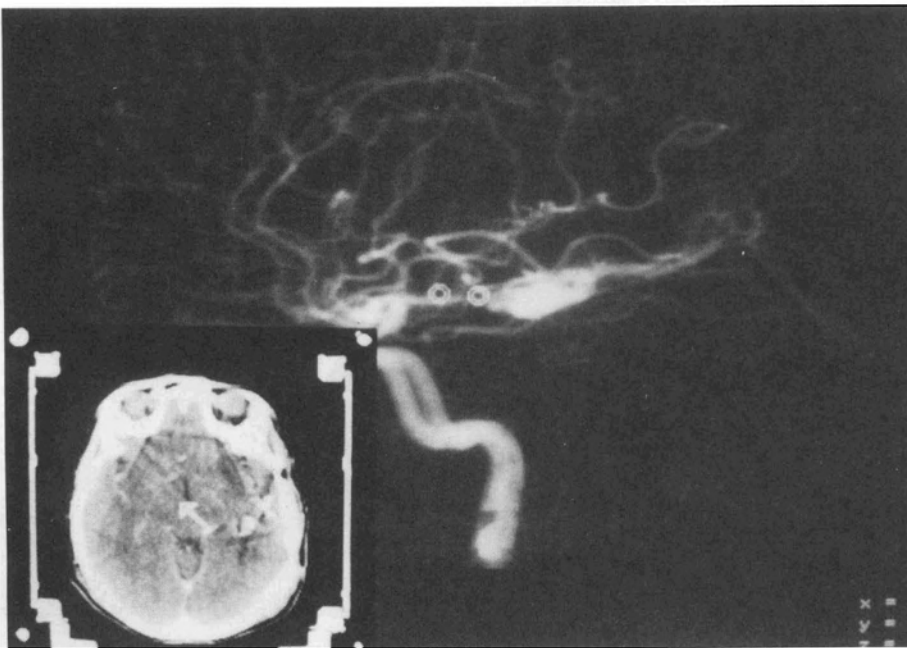


Figure 2

Figure 4 is a stereoscopic pair of images in which the information from a stereoscopic pair of DSA images has been combined with a 3-D volume reconstruction of the patient's MR data. In this case the MR data set must be volume-rendered from precisely the same viewpoint as the stereo DSA pair.

Figure 5 shows a cranio-caudal projection of an MR angiogram. This is fundamentally a 3-D image (as opposed to the 2-D projections of conventional and digital angiography) and may be viewed by the operator from any direction. It may also be readily merged with MR anatomical images, as shown in Figure 6, where we see the surface veins on the 3-D cortical MR image. We believe that images of this nature represent the state-of-the-art with respect to MR angiography.

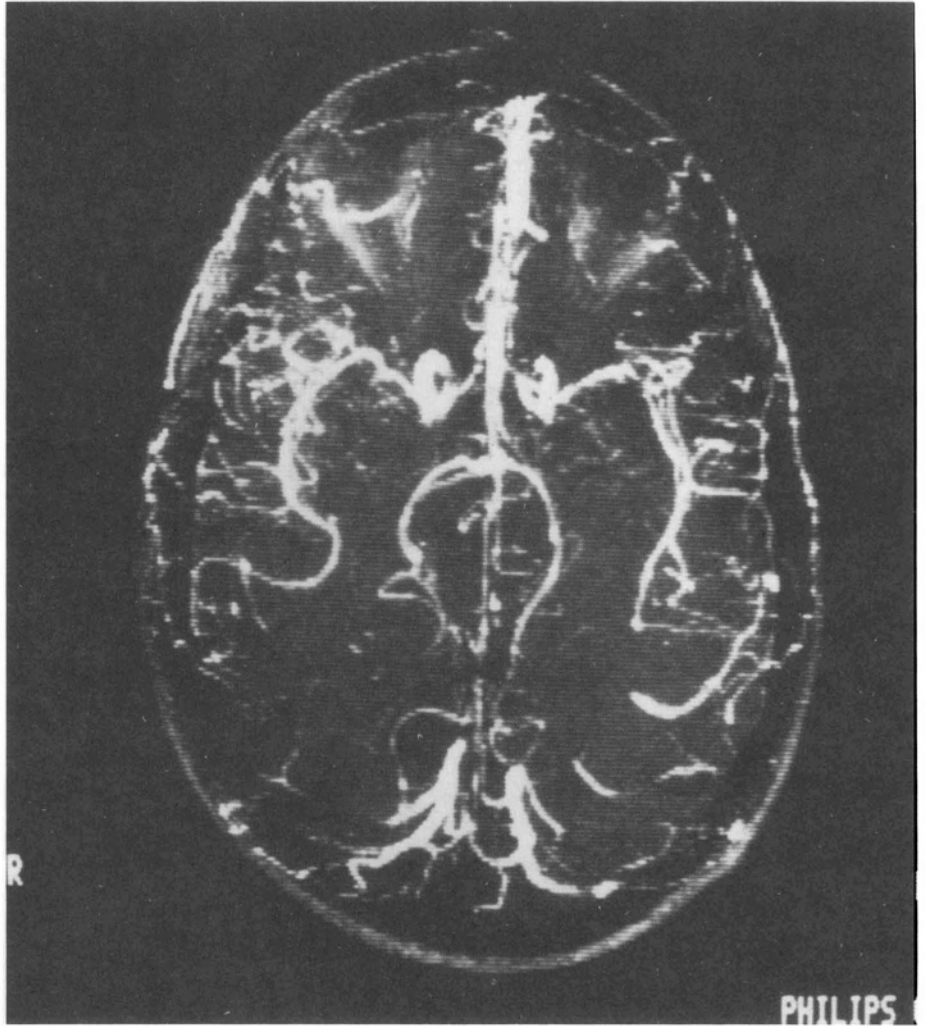
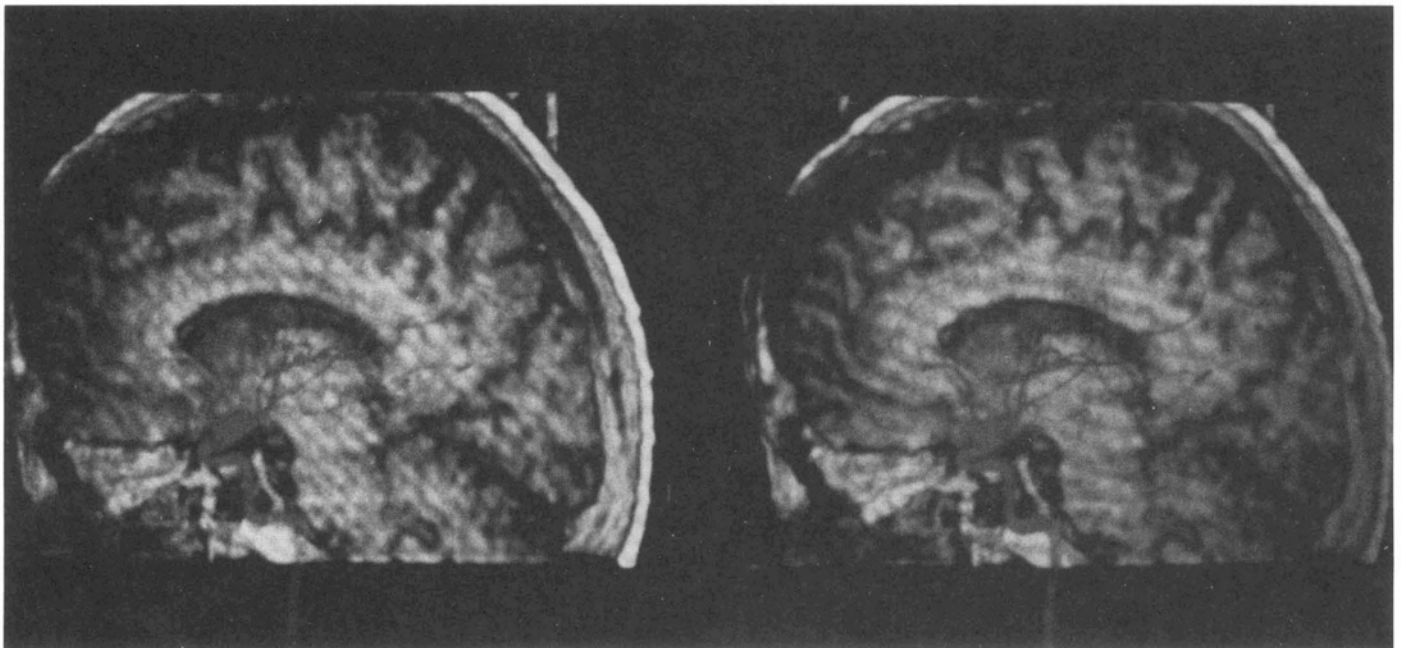


Figure 5

Figure 4



Discussion

This technique for combining data from different modalities is new and constitutes the first step towards the realization of a true 3-D workstation for the planning of stereotactic surgical procedures. It is envisaged that in its ultimate form, the surgeon will interact with the image using a hand-held 3-D localizing probe to stimulate the intended direction of approach. Stereotactic localization demands a high degree of measurement

accuracy, and we have made an extensive study of this issue with respect to the raw images obtained from each of the modalities. We have demonstrated that we may rely on the measured values to within an accuracy of 1mm in DSA, and transverse CT and MRI. Our initial experience, along with the enthusiasm of our radiological and neurosurgical colleagues, leads us to believe that a system with the capabilities described here will be a valued addition to the tools used by the neurosurgical community.

References

1. Peters TM, Clark JA, Olivier A, *et al.* Integrated stereotaxic imaging with CT MR imaging and Digital Subtraction Angiography. *Radiology* 1986;161:821-826.
2. Peters TM, Clark JA, Pike B, *et al.* Stereotactic neurosurgery planning on a personal-computer based workstation. *J Digital Imaging* 1989; 75-81.
3. Peters TM, Clark J, Pike B. A Personal-computer based workstation for the planning of stereotactic neurosurgical procedures. In: Kelly P ed. *Computers in stereotactic neurosurgery*. Boston: Blackwell Scientific Publication Inc, 1990.

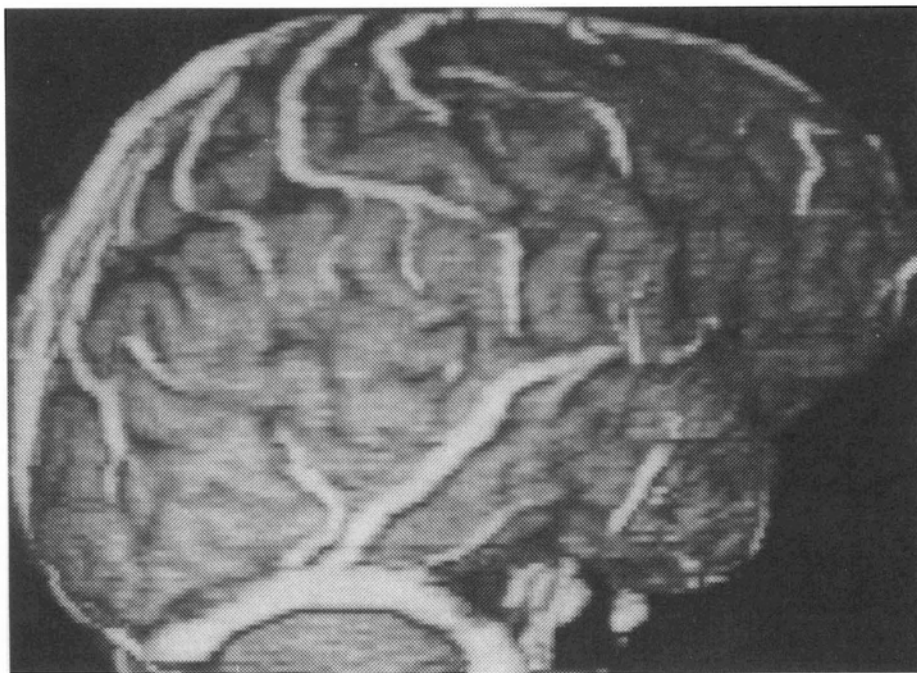


Figure 6

Reflections on Pseudotumor Cerebri

D. Melançon

This syndrome is known for its association of headaches and optic disc edema in young obese females. Optic disc edema is known to exist when raised intracranial pressure is transmitted within the optic nerve sheath.

The optic nerve sheath is patent to CSF circulation in only 1/3 patient (33%). **Fig.1**

Thus, pseudotumor cerebri may exist in young obese females with headaches, without edema of the optic disc.

And consequently, very small lateral ventricles in a female with headaches should draw attention to this syndrome even in the absence of optic disc edema. **Fig.2**

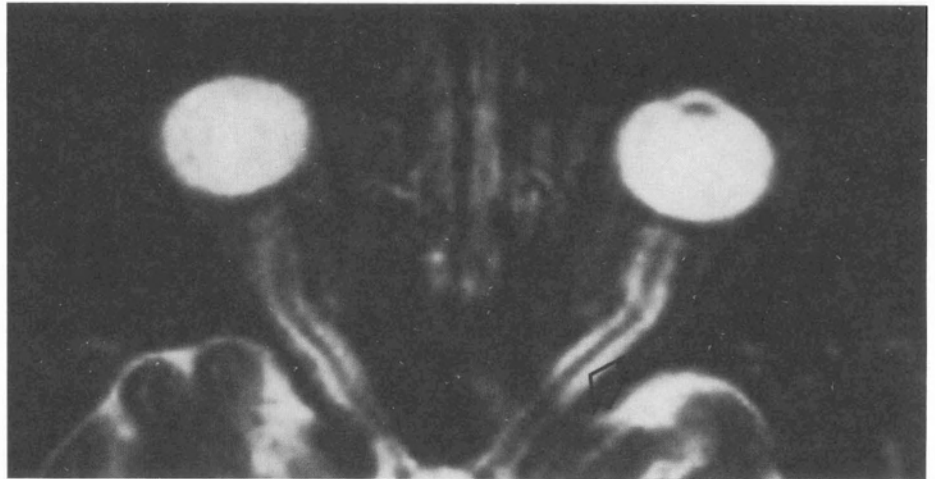


Figure 1

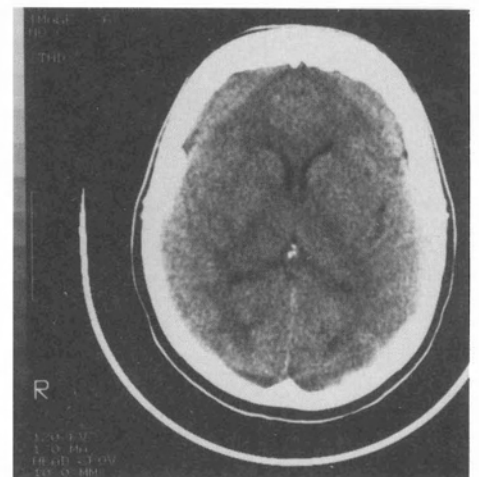
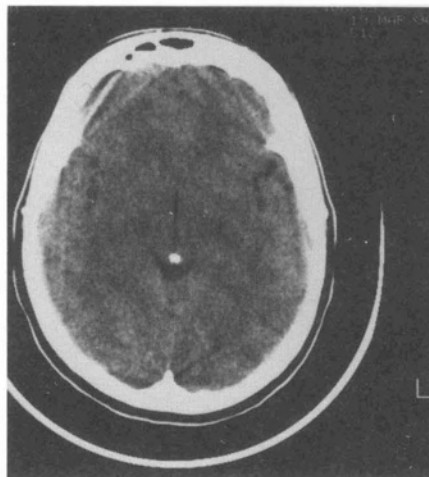


Figure 2

Glial Tumors CT Specificity

Figure 1 - An oligodendrolioma usually has multiple curvilinear calcifications associated with medium low density, usually in the paraventricular regions (frontal-occipital), and with a moderate mass effect.

Figure 2 - A gemistocytic astrocytoma is typically an iso to high density lesion, with moderate edema and mass effect, usually located in the temporal or frontal parts of the cerebral hemisphere.

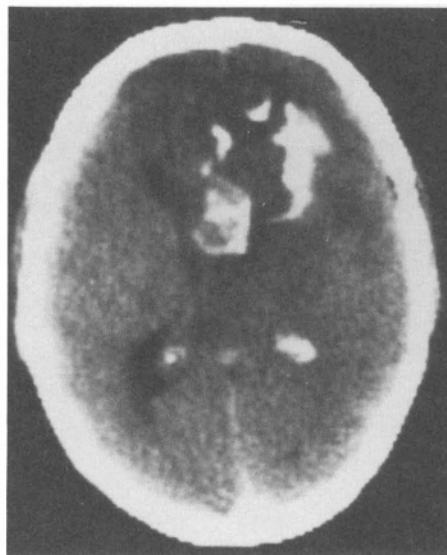


Figure 1

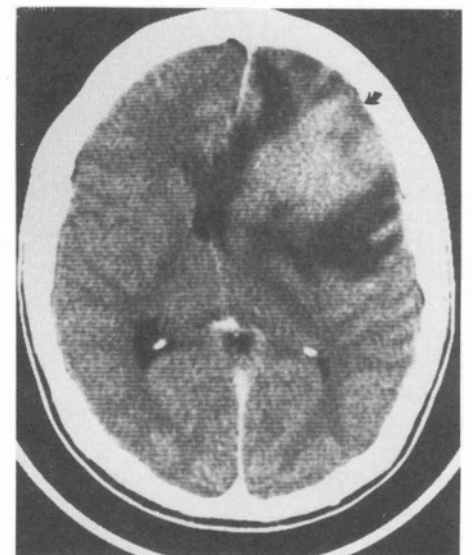


Figure 2

The Brain

...One enormous question is the working of the human brain, the most complex piece of matter we're ever likely to encounter. The three pounds of human brain is much more complex than all the trillions upon trillions of tons of matter that constitute a star. It's possible that artificial intelligence may one day develop a model of the brain; we must not underestimate the task involved. Computers do some things better than human brains. They solve mathematical problems infinitely faster and more accurately than the human brain. But that means nothing. Nobody thinks that a pocket calculator is more intelligent than a human being because it gives fast, accurate answers involving logarithms and trigonometric functions. Most human brains have difficulty even with simple arithmetic, let alone higher math. We've needed help from the very start: by counting on fingers, by using an abacus, by inventing symbols for numerals. We made mechanical calculators and ended up with electronic computers, and perhaps we'll have fancier things too, all designed to do what the human brain can't do by itself. It's enough that it can design the aids. What is it then that the human brain can do best? Those things we call intuition, insight, imagination, fantasy, creativity. We don't know how any of these work; we haven't the faintest idea how the brain does them. It's extremely important, though, to find out. Consider the magnitude of the task. The brain has 10 billion neurons and 90 billion glial cells supporting it, about 100 billion cells altogether. The computer doesn't exist that has 100 billion on/off units. Maybe someday we'll achieve that, but then there's another thing about the brain: each neuron is connected to anywhere from a dozen to a thousand other neurons in an extremely complex interrelationship that we don't understand in the least: not why it exists, not how it exists, not even remotely what it does... ..

Isaac Asimov, Radiology Today, November 1989

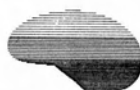
This Bulletin is sponsored by



Winthrop



HEALTH SCIENCES
DIVISION



NEURIKON

Volume 7- Numéro 1- Proceedings of NEURIKON, Dépôt légal: Bibliothèque nationale, ISSN 1180-0844, Rédacteur en chef: Denis Melançon, m.d. Ont collaboré à ce numéro: Raquel del Carpio-O'Donovan, Hoang Duong, T.M. Peters, C. Henri, L. Collin, B. Pike, A. Oliver, Isaac Asimov. Conception, réalisation: François Melançon et Barbara Kornaga. Production: Barbara Kornaga (514) 845-7710.